

Part I: Boundary perturbations caused by small conductivity inhomogeneities nearly touching the boundary [joint with M. Asch, H. Kang]

Part II: T-scan Electrical Impedance Imaging system [joint with O. Kwon, J.K. Seo, E. Woo]

Boundary perturbations caused by small conductivity inhomogeneities [joint with M. Asch, H. Kang]

$\Omega \subset \mathbb{R}^2$ : Lipschitz bounded domain. Suppose that  $\Omega$  contains a conductivity inhomogeneity  $D = z + \epsilon B$ ,  $B$  Lipschitz bounded domain.

$\text{dist}(z, \partial\Omega) = M\epsilon$ ,  $M$ : fixed positive constant.

$D$ : Nearly touching the boundary.

The conductivity of  $\Omega \setminus \overline{D} = 1$ ; the conductivity of  $D = k$ ,  $0 < k \neq 1 < +\infty$ .

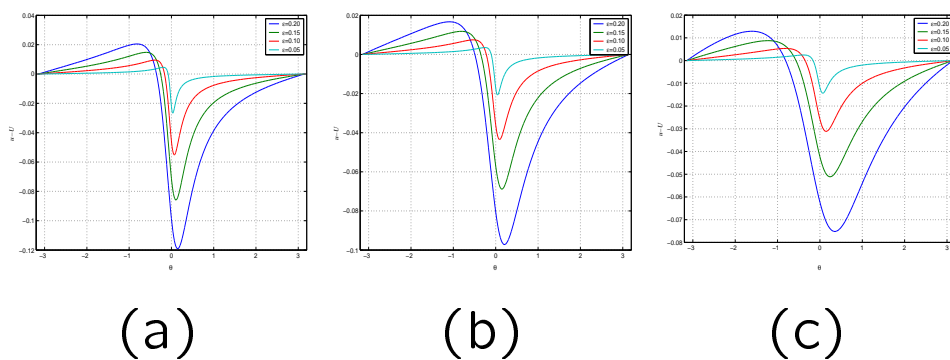
$u$ : voltage potential

$$\begin{cases} \nabla \cdot \left( 1 + (k - 1)\chi(D) \right) \nabla u = 0 & \text{in } \Omega, \\ \frac{\partial u}{\partial \nu} \Big|_{\partial\Omega} = g \in L_0^2(\partial\Omega), \\ \int_{\partial\Omega} u = 0, \end{cases}$$

$U$ : the solution of the conductivity problem in the absence of any inhomogeneity.

## Numerical computations by direct simulations

$u - U$ : leading order boundary perturbations resulting from  $D$ .



$k = 2$  and  $\epsilon$  varying with (a)  $M = 1.5$ , (b)  $M = 2$  and (c)  $M = 3$ . Colors: blue  $\epsilon = 0.2$ ; green  $\epsilon = 0.15$ ; red  $\epsilon = 0.1$  and cyan  $\epsilon = 0.05$ .

- Perturbation peak corresponds to the position of the conductivity inclusion

- Peak sharper as  $M$  decreases
- Perturbation amplitude is asymptotically **first order** in  $\epsilon$  near the inclusion while it is  $O(\epsilon^2)$  far away

⇒ **Significant change** in the voltage potentials when the inclusion is brought in close to the boundary

### Key idea

When the inclusion is not too close to the boundary it can be modeled by a **dipole** (because the potential within the inclusion is **nearly constant**). On decreasing the inclusion-boundary separation, this assumption begins to fail because **higher-order multipoles** become significant due to the inclusion-boundary interaction.

**Objective:** Derive **mathematically rigorous formula** for the leading order boundary perturbations  $(u - U|_{\partial\Omega})$  resulting from  $D$

**Motivation:** Motivated by the inverse problem of determining the **location** and some **geometric features** of  $D$  from the **peak**: **Design non-iterative real-time algorithms for imaging  $D$** ; extract some core information on the conductivity inclusion  $D$ .

Fundamental limitations of EIT (ill-posedness and nonlinearity)  $\Rightarrow$  not possible to reconstruct the exact shape of  $D$  and its exact conductivity (**high frequency information** from **zero frequency data**).

Asymptotic formula when  $D$  is not too close to the boundary  $\partial\Omega$  [A. Friedman, M. Vogelius, S. Moskow, D. Volkov, H. Kang, J.K. Seo, H.A.]

$$(u - U)(x) = \epsilon^2 \nabla U(z)^T M \nabla N(x, z) + o(\epsilon^3)$$

holds uniformly on  $\partial\Omega$

Dipole approximation

N: Neumann function

$$\begin{cases} \Delta_x N(x, z) = -\delta_z & \text{in } \Omega, \\ \frac{\partial N}{\partial \nu_x} \Big|_{\partial\Omega} = -\frac{1}{|\partial\Omega|} \\ \int_{\partial\Omega} N(x, z) d\sigma(x) = 0 & \text{for } z \in \Omega. \end{cases}$$

M: Polarization tensor: two equivalent definitions

Variational definition:

$$M = (k - 1)(I + (k - 1) \int_B \nabla \Psi)$$

$$\left\{ \begin{array}{l} \Delta \Phi = 0, \quad B \cup (\mathbb{R}^2 \setminus \overline{B}) , \\ \Phi \Big|_+ - \Phi \Big|_- = 0, \quad \partial B , \\ \frac{\partial \Phi}{\partial \nu} \Big|_+ - k \frac{\partial \Phi}{\partial \nu} \Big|_- = \nu \quad \partial B , \\ \lim_{|\xi| \rightarrow +\infty} \Phi = 0. \end{array} \right.$$

Via layer potential techniques:

$G(x) = 1/2\pi \ln |x|$ : the fundamental solution of  $\Delta$  in  $\mathbb{R}^2$

**Simple** and **double-layer potentials** of a density  $\phi$ , on  $\partial D$ ,  $D$  bounded Lipschitz domain,

$$\mathcal{S}_B \phi(x) := \int_{\partial B} G(x-y) \phi(y) d\sigma_y, \quad x \in \mathbb{R}^2,$$

$$\mathcal{D}_B \phi(x) := \int_{\partial B} \frac{\partial}{\partial \nu_y} G(x-y) \phi(y) d\sigma_y, \quad x \in \mathbb{R}^2 \setminus \partial B.$$

Trace formulae [Verchota]:

$$\begin{aligned}\frac{\partial}{\partial \nu^\pm} \mathcal{S}_B \phi(x) &= (\pm \frac{1}{2} I + \mathcal{K}_B^*) \phi(x), \\ (\mathcal{D}_B \phi)|_\pm &= (\mp \frac{1}{2} I + \mathcal{K}_B) \phi(x), \quad x \in \partial B,\end{aligned}$$

$$\mathcal{K}_B \phi(x) = \frac{1}{\omega_d} \text{p.v.} \int_{\partial B} \frac{\langle x - y, \nu_y \rangle}{|x - y|^2} \phi(y) d\sigma_y$$

$\mathcal{K}_B^*$  is the adjoint of  $\mathcal{K}_B$  in  $L^2(\partial B)$ .

[Verchota]  $\frac{1}{2}I - \mathcal{K}_B^* : L_0^2(\partial B) \rightarrow L_0^2(\partial B)$  is an isomorphism

[Escauriaza-Fabes-Verchota]  $|\lambda| > 1/2$ ,  $\lambda I - \mathcal{K}_B^* : L^2(\partial B) \rightarrow L^2(\partial B)$  is an isomorphism.

$$M = \int_{\partial B} (\lambda I - \mathcal{K}_B^*)^{-1}(\nu) y d\sigma(y)$$

$$\lambda = \frac{k+1}{2(k-1)}, \quad 0 \leq k \neq 1 \leq +\infty$$



Properties of the Polarization tensor [G. Pólya, G. Szegő, R.E. Kleinman, V. Mazzy'a, A.B. Movchan, H.Kang, H.A.]

Symmetry, positivity, isoperimetric inequalities  
( $Tr(M) \simeq \lambda|B|$ )

M occurs in several other interesting contexts

↪ Low-frequency scattering

↪ **Dilute composites**: effective electrical conductivity of two-phase medium consisting of inclusions of one material of known shape embedded into a matrix of another having  $\neq$  conductivity [joint with H. Kang, K. Touibi]

Generalization of the Maxwell-Garnett formula:

$$\tilde{k} = I + fM + f^2M^2 + \begin{cases} O(f^3) & \text{symmetric } B \\ O(f^{\frac{5}{2}}) & \text{general case} \end{cases}$$

f: volume fraction

M admits a natural generalization [joint with H. Kang]

Generalized polarization tensors

$$M^{\alpha\beta} = \int_{\partial B} (\lambda I - \mathcal{K}_B^*)^{-1} \left( \frac{\partial y^\alpha}{\partial \nu} \right) y^\beta d\sigma(y), \alpha, \beta \in \mathbb{N}^2$$

Basic building blocks for higher-order asymptotic expansions of  $u - U$  on  $\partial\Omega \hookrightarrow$  higher-order multipoles

Symmetry, positivity, isoperimetric inequalities

$$u - U = \epsilon^2 \nabla U(z)^T M \nabla N(x, z) + o(\epsilon^3)$$

Quantify the remainder  $o(\epsilon^3)$  [joint with J.K. Seo]

$$o(\epsilon^3) \sim C\epsilon^3$$

$C$  blows up when  $\text{dist}(D, \partial\Omega) \rightarrow 0$  and when  $B$  has a bad Lipschitz character ( $B$  becomes flat)  
 $\Rightarrow$  Not valid expansion

$D$  thin inhomogeneity: E. Beretta, E. Francini, M. Vogelius

$$\text{dist}(D, \partial\Omega) \rightarrow 0$$

**Theorem** Let  $z_0$  be the projection of  $z$  on  $\partial\Omega$ . Suppose that  $g \in \mathcal{C}^1(\partial\Omega)$  and  $\Omega$  is of class  $\mathcal{C}^2$ . The following asymptotic expansion holds uniformly on  $\partial\Omega$ :

$$\begin{aligned} (u - U)(x) = & -\epsilon \nabla U(z_0) \cdot \left( \int_{\partial B} N(x, z + \epsilon y) (\lambda I - \mathcal{K}_B^*)^{-1}(\nu) d\sigma_y \right) \\ & - \epsilon \frac{W(x)}{1 - W(z_0)} \nabla U(z_0) \\ & \cdot \left( \int_{\partial B} N(z_0, z + \epsilon y) (\lambda I - \mathcal{K}_B^*)^{-1}(\nu) d\sigma_y \right) \\ & + O(\epsilon^{3/2}). \end{aligned}$$

If  $|x - z_0| \gg O(\epsilon)$  then

$$\begin{aligned} (u - U)(x) = & -\epsilon^2 \nabla U(z_0)^T M \nabla N(x, z_0) \\ & - \epsilon \frac{W(x)}{1 - W(z_0)} \nabla U(z_0) \\ & \cdot \left( \int_{\partial B} N(z_0, z + \epsilon y) (\lambda I - \mathcal{K}_B^*)^{-1}(\nu) d\sigma_y \right) \\ & + O(\epsilon^{5/2}), \end{aligned}$$

where  $M = \int_{\partial B} y(\lambda I - \mathcal{K}_B^*)^{-1}(\nu) d\sigma_y$  is the polarization tensor and  $N$  is the Neumann function.

$W(x)$  describes the effect due to the interaction between the inclusion and the boundary.

Since

$$\int_{\partial B} N(x, z + \epsilon y)(\lambda I - \mathcal{K}_B^*)^{-1}(\nu) d\sigma_y = O(1)$$

for  $x$  near  $z_0 \Rightarrow (u - U)(x) = O(\epsilon)$  near  $z_0$ , while  $(u - U)(x) = O(\epsilon^2)$  for  $x$  far away from  $z_0$ . Thus  $u - U$  has a relative peak near  $z_0$ .

Proof of the Theorem:

- Energy estimates by the Rellich identity.
- Technical estimates on Poisson-type kernels.

**Lemma** Suppose that  $\partial\Omega$  is of class  $\mathcal{C}^2$  and  $D = \epsilon B + z$ . Let  $z_0$  be the normal projection of  $z$  onto  $\partial\Omega$ . Define

$$w(x) := \frac{\epsilon}{(z_0 - x) \cdot \nu_{z_0}}, \quad x \in \partial D.$$

For  $f \in \mathcal{C}^0(\partial\Omega)$ , let

$$s_f(\epsilon) := \sup_{|x - z_0| \leq \epsilon} |f(x) - f(z_0)|.$$

Then,

$$\sup_{x \in \partial D} |\epsilon \nabla \mathcal{D}_\Omega(f)(x) + w(x)f(z_0)\nu_{z_0}| \leq C(s_f(\sqrt{\epsilon}) + \sqrt{\epsilon})\|f\|_{L^\infty(\partial\Omega)},$$

where  $C$  is independent of  $\epsilon$  and  $f$ .

$$W(x) := \nu_{z_0} \cdot \int_{\partial D} \frac{N(x, y) - N(x, z)}{\epsilon} (\lambda I - \mathcal{K}_D^*)^{-1}(w\nu),$$

$x \in \partial\Omega$ .

## A Unit Disk Containing a Single Disk-Shaped Imperfection: A Numerical Example

$$(\lambda I - \mathcal{K}_D^*)^{-1}(\nu)(y) = \frac{1}{\lambda} \nu_y, \forall y \in \partial\Omega$$

$$N(x, y) = -2\Gamma(x - y) \text{ modulo constants, } \forall x \in \partial\Omega, y \in \Omega$$

$$g(1, \theta) = \cos \theta + \sin \theta.$$

$$U(r, \theta) = r(\cos \theta + \sin \theta).$$

$(u - U)(z_0)$  can be approximated as follows:

$$(u - U)(z_0) \simeq -\frac{\epsilon(k - 1)}{\pi(k + 1)(1 - W(z_0))} \int_0^{2\pi} \log \left( (M - \cos \theta)^2 + \sin^2 \theta \right) (\cos \theta + \sin \theta) d\theta$$

$$W(z_0) = \frac{1 - k}{2\pi(k + 1)} \int_0^{2\pi} \log \left( \frac{(M - \cos \theta)^2 + \sin^2 \theta}{M^2} \right) \frac{\cos \theta}{M - \cos \theta} d\theta$$

	$M = 3.0$	$M = 4.0$	$M = 5.0$
$\epsilon = 0.05$	0.0118	0.0093	0.0076
	0.0116	0.0085	0.0068
$\epsilon = 0.02$	0.0046	0.0035	0.0028
	0.0046	0.0034	0.0027
$\epsilon = 0.01$	0.0023	0.0017	0.0014
	0.0023	0.0017	0.0014

Comparison of  $(u - U)(z_0)$  computed numerically (upper lines) and  $(u - U)(z_0)$  computed from the asymptotic formula (lower lines) for  $k = 2$ .

## Precise dependence with respect to $k$ and $M$

↪ Design an **efficient algorithm** for reconstructing  $z_0, M, \epsilon, k$  (can not separate between  $k$  and  $\epsilon$ )



## Half space problem [joint with H. Kang]

Simpler formula

$$\begin{cases} \nabla \cdot (1 + (k - 1)\chi(D))\nabla u = 0 & \text{in } \mathbb{R}_-^2, \\ \frac{\partial u}{\partial x_2} \Big|_{\partial \mathbb{R}_-^2} = g \in L_0^2(\partial \mathbb{R}_-^2). \end{cases}$$

Weighted Sobolev spaces

Let  $\Phi_i^-$  be the unique solution to

$$\begin{cases} \Delta \Phi_i^- = 0, & B \cup (\mathbb{R}_-^2 \setminus \overline{B}), \\ \frac{\partial \Phi_i^-}{\partial \xi_2} = 0, & \partial \mathbb{R}_-^2, \\ \Phi_i^- \Big|_+ - \Phi_i^- \Big|_- = 0, & \partial B, \\ \frac{\partial \Phi_i^-}{\partial \nu} \Big|_+ - k \frac{\partial \Phi_i^-}{\partial \nu} \Big|_- = \nu_i & \partial B, \\ \lim_{\xi_2 \rightarrow -\infty} \Phi_i^- = 0. \end{cases}$$

$$\Phi^{-} = \begin{pmatrix} \Phi_1^{-} \\ \Phi_2^{-} \end{pmatrix}$$

$$u(x) = U(x) + (k - 1)\epsilon^2 \nabla U(z_*).$$

$$\left( \int_B \nabla N(x, \epsilon y + z) \cdot (I + (k - 1) \nabla_y \Phi^{-}(y)) \, dy \right) \\ + O(\epsilon^3), \quad x \in \partial \mathbb{R}_-^2.$$

$$\int_B \nabla N(x, \epsilon y + z) \cdot \nabla_y \Phi^{-}(y) \, dy \\ = 2 \int_B \nabla \Gamma(x - \epsilon y - z) \cdot \nabla_y \Phi^{-}(y) \, dy, \quad x \in \partial \mathbb{R}_-^2$$

Expanding  $\nabla \Gamma(x - \epsilon y - z)$  as  $\epsilon$  goes to zero yields the following theorems.

**Theorem 1** For any  $x \in \partial \mathbb{R}_-^2$ :  $|x - z_*| \gg \epsilon$ ,

$$u(x) = U(x) + 2\epsilon^2(k - 1)\nabla U(z_*). \\ \left( |B|I + (k - 1) \int_B \nabla_y \Phi^{-}(y) \, dy \right) \nabla_z \Gamma(x - z_*) \\ + O(\epsilon^3).$$

$(k-1)(I + (k-1) \int_B \nabla_y \Phi^-(y) dy)$ : half space polarization tensor

**Theorem 2** For any  $x \in \partial\mathbb{R}_-^2$ :  $|x - z_*| = O(\epsilon)$ , we have

$$(u - U)(x) = -\frac{\epsilon}{2\pi}(k-1)\nabla U(z_*) \cdot \int_{\partial B} \ln((d_{z_*}(x) - y_1)^2 + (M - y_2)^2) \frac{\partial((k-1)\Phi^- + y)}{\partial\nu} \Big|_- + O(\epsilon^2),$$

where  $d_{z_*}(x) = (x - z_*)_1/\epsilon$  (scaled distance) and  $\epsilon M = |z - z_*|$ .

The two asymptotic expansions match in some overlap region

$$\begin{aligned}
& \int_{\partial B} \ln((d_{z_*}(x) - y_1)^2 + (\alpha - y_2)^2) \frac{\partial \Phi^-}{\partial \nu} \Big|_- (y) d\sigma(y) \\
&= -\frac{2}{d_{z_*}(x)} \int_{\partial B} y_1 \frac{\partial \Phi^-}{\partial \nu} \Big|_- (y) d\sigma(y) \\
&+ O\left(\frac{1}{d_{z_*}(x)^2}\right) \quad \text{as } d_{z_*}(x) \rightarrow +\infty,
\end{aligned}$$

Connection between the half-space and whole space polarization tensors

$B^+$ : the reflection of  $B$  with respect to  $y_2 = 0$ .

$$\left\{ \begin{array}{l} \Delta \Phi = 0, \quad B \cup B^+ \cup (\mathbb{R}_-^2 \setminus (\overline{B} \cup \overline{B}^+)) , \\ \Phi \Big|_+ - \Phi \Big|_- = 0, \quad \partial(B \cup B^+) , \\ \frac{\partial \Phi}{\partial \nu} \Big|_+ - k \frac{\partial \Phi}{\partial \nu} \Big|_- = \nu \quad \partial(B \cup B^+) , \\ \lim_{|\xi| \rightarrow +\infty} \Phi = 0. \end{array} \right.$$

$(k-1)(I + (k-1) \int_{B \cup B^+} \nabla_y \Phi(y) dy)$ : whole space  
PT

↪ Equivalent ellipse with the same polarization tensor (general result for multiple inclusions [joint with [H. Kang](#), [E. Kim](#), [M. Lim](#)] : equivalent ellipse with overall conductivity)

$$(2 \int_B \nabla_y \Phi^-(y) dy)_{11} = (\int_{B \cup B^+} \nabla_y \Phi(y) dy)_{11}$$

$$(2 \int_B \nabla_y \Phi^-(y) dy)_{12} = 0$$

## T-scan Electrical Impedance Imaging system

[joint with O. Kwon, J.K. Seo, E. Woo]

- **Breast cancer** is the most common form of cancer in women - one out of nine women will develop breast cancer in her lifetime. About 200,000 women in the U.S. will be diagnosed with breast cancer each year, and about 40,000 women will die from this disease each year.
- **X-ray mammography** is recognized as the "gold standard" for breast cancer detection. Mammographic **sensitivity and specificity are low** for young women and those with dense breast tissue.
- Mammography is not recommended for screening in young women due to its reduced sensitivity and specificity in dense breast tissue

and concern about increased lifetime exposure to radiation.

- Mammography has an overall 25% false positive rate which leads to unnecessary biopsies. 85% of mammography initiated biopsies are negative.
- MRI suffers from the limitations of high expense, **reduced sensitivity for small carcinomas**, and reduced specificity in particular as a result of hormonal factors. Currently these exams may not be suitable for widespread, population-based screening.
- **Breast ultrasound** uses high-frequency waves to image the breast. Ultrasound does not have good spatial resolution and also unable to image micro-calcifications, tiny calcium deposits that are often the first indication of breast cancer.

- **Electrical Impedance Technology** is based on the discovery that normal and malignant breast tissues have **different electrical properties**.
- The T-Scan 2000ED generates a low-level electric signal that is transmitted into the body. The resulting electric field is then measured by sensors in a non-invasive probe placed on the breast. Measurements are made over several frequencies using proprietary algorithms to create and display a real-time electrical image of the breast along with immediate results.
- **Benefits of the T-Scan 2000ED**
  - Safe and radiation-free
  - Painless exam



Real-time imaging

Portable

- Previous results

Assenheimer et al. (Physiol. Meas., 2001) found an expression showing the relation between the amount of field distortion at the plane of  $z=0$  and anomaly information. It is difficult to quantitatively estimate its accuracy and perform any further analysis.

B. Scholz (IEEE Trans. Med. Imag, 2002) presented an approximate expression for trans-admittance data at  $z=0$  using lead vectors regarding the anomaly as multipolar signal sources. However, the expression lacks of generality and flexibility.

In order to develop a more accurate anomaly estimation algorithm capable of error analysis, an explicit representation of the relation between the measured trans-admittance data and anomaly information is required.

- Difficulties

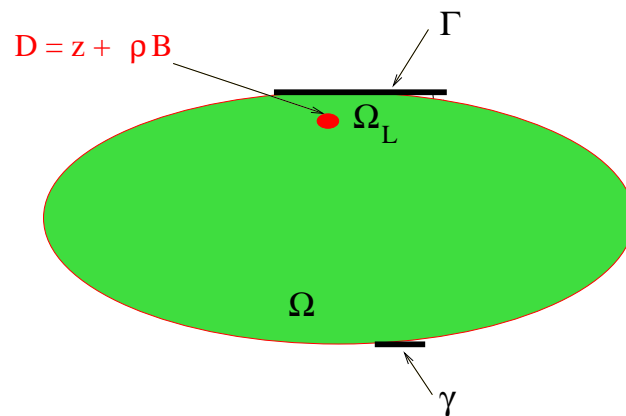
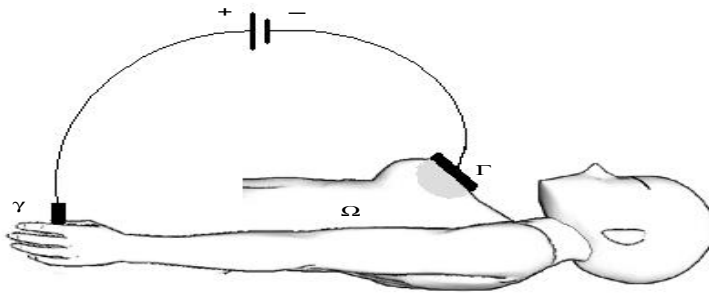
We only measure the data in a **small portion** instead of the whole surface.

Electrical safety regulations limit the amount of total current flowing through the human subject and therefore the range of the **applied voltage** is also **limited**.

Since the breast differs for each subject, our detection algorithm should **not depend much on the global geometry** of the breast.

**Breast is not homogeneous.**

## T-scan: Mathematical model



$E_\rho$ : voltage potential

$$\begin{cases} \nabla \cdot (\sigma + i\omega\epsilon)\nabla E_\rho = 0 & \Omega, \\ E_\rho = 0 & \Gamma, \quad E_\rho = 1 & \gamma, \\ \frac{\partial E_\rho}{\partial \nu} = 0 & \partial\Omega \setminus \Gamma \cup \gamma. \end{cases}$$

Suppose

$$\sigma + i\omega\epsilon = \begin{cases} \tau_1 := \sigma_1 + i\omega\epsilon_1 & \text{in } \Omega_L \setminus D \\ \tau_2 := \sigma_2 + i\omega\epsilon_2 & \text{in } D. \end{cases}$$

Key idea

- Keeping  $E_\rho = 0$  on  $\Gamma$  has a **great advantage** because forces the level surface of the voltage in the breast region to be approximately parallel to the probe and  $\nabla E_\rho$  will be in the direction perpendicular to the level surface. Since the conductivity of  $D$  is much higher than the surrounding, more currents will flow along  $D$ . This enables us to guess that  $D$  may exist below the point where  $g$  has a maximum.
- Applications of several highly oscillatory voltages on the small portion  $\Gamma$  as is done in

most EIT techniques may not have much advantage to localize  $D$  below  $\Gamma$  with a certain depth.

$E_\rho$  satisfies in  $\Omega_L$  :

$$\nabla \cdot \left( \tau_1 \chi(\Omega_L \setminus \overline{D}) + \tau_2 \chi(D) \right) \nabla E_\rho = 0 \quad \text{in } \Omega_L.$$

Set

$$\tau_1 \frac{\partial E_\rho}{\partial \nu} = g, \tau_2 \frac{\partial E_0}{\partial \nu} = g^0, \quad \text{on } \Gamma.$$

$$g_L = \tau_1 \frac{\partial E_\rho}{\partial \nu}, f_L = E_\rho, g_L^0 = \tau_1 \frac{\partial E_0}{\partial \nu}, f_L^0 = E_0 \quad \text{on } \partial\Omega_L.$$

Prove  $\forall x \in \mathbb{R}^3 \setminus \overline{\Omega_L}$  :

$$\begin{aligned} (\tau_1 - \tau_2) \int_D \nabla_y E_\rho(y) \cdot \nabla_y G(x - y) dy = \\ \mathcal{S}_{\partial\Omega_L}(g_L - g_L^0)(x) + \tau_1 \mathcal{D}_{\partial\Omega_L}(f_L - f_L^0)(x). \end{aligned}$$

$\Gamma$  planar surface (great advantage of using a probe with a planar array of electrodes):

$$\begin{aligned} & (\tau_1 - \tau_2) \frac{\partial}{\partial z} \int_D \nabla_y E_\rho(y) \cdot \nabla_y G(x - y) dy \\ &= \frac{1}{2}[g(x) - g^0(x)] + \Xi(x), \quad x \in \Gamma, \end{aligned}$$

$$\begin{aligned} \Xi(x) &:= \frac{\partial}{\partial z} \mathcal{S}_{\partial\Omega_L \setminus \Gamma}[g_L - g_L^0](x) \\ &+ \tau_1 \frac{\partial}{\partial z} \mathcal{D}_{\partial\Omega_L \setminus \Gamma}[f_L - f_L^0](x), \quad x \in \Gamma. \end{aligned}$$

$\forall x \in \Gamma$  :

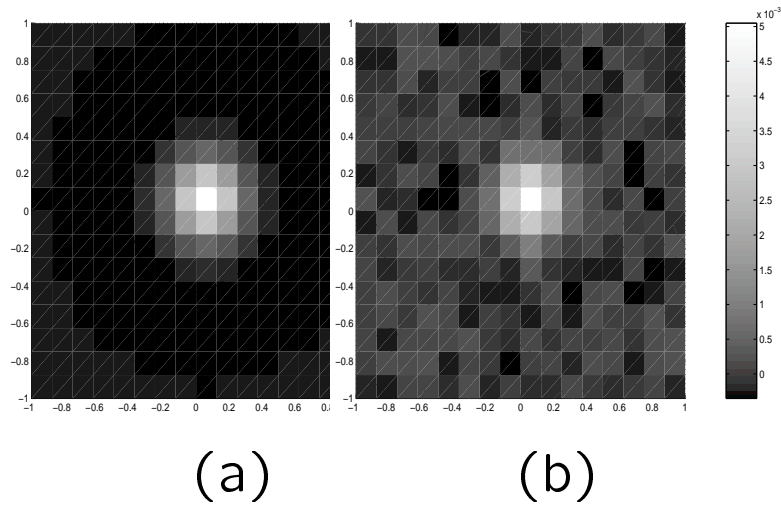
$$\begin{aligned} \frac{1}{2}[g - g^0](x) &\approx (\tau_1 - \tau_2) \frac{\partial}{\partial z} \left( \frac{x - z}{4\pi|x - z|^3} \right) \\ &\cdot \int_D \nabla E_\rho(y) dy. \end{aligned}$$

Approximating

$$\int_D \nabla E_\rho(y) dy \approx \frac{-3\bar{g}^0|D|}{2\tau_1 + \tau_2} \vec{e}_3,$$

where  $\bar{g}^0$  denotes the average of  $\bar{g}^0$ , we arrive at  $\forall x \in \Gamma$  :

$$\frac{1}{2}[g - g^0](x) \approx \frac{3\bar{g}^0(\tau_1 - \tau_2)}{2\tau_1 + \tau_2} |D| \frac{\partial^2}{\partial z^2} \frac{1}{4\pi|x - z|}.$$



intensity of  $|g - g^0|$ ; (a) 0% of noise; (b) 5% of noise

The brightness of the image indicates the amplitude of  $|g - g^0|$ .

## Multi-frequency Reconstruction Algorithm

	10 KHz		100KHz	
	Normal	Cancer	Normal	Cancer
	0.03	0.2	0.03	0.2
$\sigma$	800	20000	100	6000
$\epsilon/\epsilon_0$				

### Detection algorithm:

- **Transversal position:** The anomaly  $D$  lies below the point  $z^*$  at which the absolute value  $|g(z^*) - \tilde{g}(z^*)|$  has the greatest quantity:

$$|g(z^*) - \tilde{g}(z^*)| = \max_{x \in \Gamma} |g(x) - \tilde{g}(x)|.$$

- **Depth:** Let  $x_0$  be any chosen point on  $\Gamma$  near  $z^*$  and let  $l$  be the distance between  $z^*$  and  $x_0$ , that is,  $l = |z^* - x_0|$ . The depth  $d$  is determined by the identity:

$$\frac{g(z^*) - \tilde{g}(z^*)}{g(x_0) - \tilde{g}(x_0)} = \frac{|2 - \frac{l^2}{d^2}|}{2(\frac{l^2}{d^2} + 1)^{5/2}}.$$



## Numerical results

Depth and size estimation for the model problem with inhomogeneous background and added random noise

	0%	2.5%	5%
−0.2 0.0625	−0.1975 0.0569	−0.1941 0.0557	−0.1821 0.0527
−0.3 0.0625	−0.2971 0.0560	−0.2929 0.0549	−0.2817 0.0533
−0.4 0.0625	−0.3918 0.0539	−0.3808 0.0526	−0.3711 0.0513

**Proof:** requires technical estimates.

**Theorem 1**  $\rho = \text{dist}(D, \Gamma)$ . The difference  $g - g_0$  on  $\Gamma$  can be expressed as

$$\frac{1}{2\mu}[g - g_0](x) = \int_D \nabla_y \left[ \frac{\partial}{\partial x_3} G(x - y) + T(x, y) \right] \cdot \nabla E_\rho(y) dy,$$

where  $T(x, y)$  satisfies the following estimate:

$$|\nabla_y T(x, y)| \leq C \rho^{-3}, \quad y \in D, x \in \Gamma.$$

**Theorem 2** Let  $z^* = (z_1, z_2, 0)$ , the projection of  $z$  on  $\Gamma$ . Then

$$\begin{aligned} \frac{1}{2}[g - g_0](x) &= g_0(z^*) \int_D \frac{\partial}{\partial x_3} \frac{(x - y) \cdot [e_3 + (\tau_2 - \tau_1) \nabla V(y)]}{4\pi|x - y|^3} dy \\ &+ Err(x), \quad x \in \Gamma, \end{aligned}$$

where the error term  $Err(x)$  satisfies the estimate:

$$|Err(x)| \leq C g_0(z^*) |D| \left( \frac{\text{diam}(D)}{\rho|x - z|^3} + \frac{1}{\rho^3} \right), \quad x \in \Gamma.$$

Here,  $V$  is the  $H^1(\Omega)$ -solution of

$$\begin{cases} \Delta V = 0 & \text{in } \Omega \setminus \partial D, \\ V^+ = V^- & \text{on } \partial D, \\ \tau_1 \frac{\partial V^+}{\partial \nu} - \tau_2 \frac{\partial V^-}{\partial \nu} = \nu \cdot e_3 & \text{on } \partial D, \\ \chi_\Gamma V + (1 - \chi_\Gamma) \frac{\partial V}{\partial \nu} = 0 & \text{on } \partial \Omega. \end{cases}$$

*D* ball:

$$\frac{1}{2}[g-g_0](x)\approx \frac{3g(z^*)(\tau_1-\tau_2)}{2\tau_1+\tau_2}|D|\frac{2z_3^2-(x_1-z_1)^2-(x_2-z_2)^2}{4\pi|x-z|^5}.$$